



**UNIVERSITY OF PADOVA**

**Department of General Psychology**

**Bachelor's Degree in Techniques and Methods in Psychological Science**

**Final dissertation**

**Heart-evoked potential to assess interoception in women with high emotional  
dysregulation**

*Supervisor*

**Prof. Dr. Marco Marino**

*Candidate: Jefimija Novakovic*

*Student ID number: 2088531*

Academic Year: 2024/2025

## **Abstract:**

Interoception, the perception of internal bodily signals, plays a central role in emotional regulation. This thesis examined heartbeat-evoked potentials (HEPs), a neural index of interoceptive processing, in women with high (HD) and low (LD) emotion dysregulation at rest, focusing on early (N1; 150–250 ms) and late (P1; 300–400 ms) components. Forty-three female participants completed EEG and ECG recordings, along with validated questionnaires of anxiety (STAI-T), impulsivity (UPPS-P), and affective lability (ALS-18). Results showed that the HD group displayed stronger early negativity (N1) and weaker late positivity (P1) compared to the LD group, consistent with heightened bottom-up interoceptive sensitivity to cardiac signals (reflected in stronger N1) but diminished top-down, evaluative control (reflected in weaker P1), suggesting an altered interoceptive hierarchy in emotionally dysregulated individuals. Within the HD group, higher scores on anxiety, impulsivity, and affective lability correlated positively with N1 amplitudes and negatively with P1 amplitudes, while these associations were absent in the LD group. Questionnaire scores were also strongly intercorrelated, supporting the view that these traits reflect overlapping aspects of emotional dysregulation. Although one positive association between heart rate variability (SDNN) and P1 amplitude emerged in the HD group, no consistent autonomic differences were found. Together, the findings suggest that an “early strong, late weak” HEP profile may index emotional dysregulation in women, pointing to HEPs as a potential physiological marker of transdiagnostic traits.

## Table of contents:

<b>Chapter 1 - Introduction</b>	5
1.1 Introduction to interoception	5
1.2 Neural pathways of interoceptive processing	5
1.3 Cardiac interoception	7
1.4 Heartbeat-Evoked Potentials (HEPs)	8
1.5 Altered interoception and emotional dysregulation	10
1.6 Interoception, emotion, and trait anxiety	11
1.7 Interoception, emotion, and impulsivity	12
1.8 Interoception, emotion, and affective lability	13
1.9 Sex differences in interoception and emotional reactivity	13
1.10 Aims and hypotheses	14
<b>Chapter 2 - Materials and Methods</b>	15
2.1 Participants and data	15
2.2 Psychometric measures	15
2.3 Physiological measurements (EEG/ECG acquisition)	16
2.3.1 EEG/ECG pre-processing	17
2.3.2 EEG/ECG processing	17
2.4 Statistical analysis	18
<b>Chapter 3 - Results</b>	19
3.1 Questionnaires	19
3.1.1 Group differences	19
3.1.2 Correlations between questionnaires	20
3.2 HEP results	21
3.2.1 Grand average and Global Field Power (GFP)	21
3.2.2 Topographical distribution	24
3.3 Cardiac physiology (ECG/HRV)	26
3.3.1 Descriptives and group differences	26
3.4 Correlational analyses	28
3.4.1 HEP and questionnaires	28
3.4.2 Impulsivity (UPPS-P) and HEP	29
3.4.3 Affective lability (ALS-18) and HEP	30
3.4.4 Trait anxiety (STAI-T) and HEP	31

3.4.5 HR, HRV, and HEP	32
3.4.6 HR, HRV, and questionnaires	33
<b>Chapter 4 - Discussion</b>	<b>35</b>
4.1 Main HEP effects	35
4.2 Trait associations	36
4.2.1 Impulsivity (UPPS-P)	36
4.2.2 Trait anxiety (STAI-T)	36
4.2.3 Affective lability (ALS-18)	37
4.3 Between-questionnaire overlap (transdiagnostic)	37
4.4 HRV context and neurovisceral integration	38
<b>Chapter 5 - Limitations</b>	<b>39</b>
<b>Chapter 6 - Conclusion</b>	<b>40</b>
<b>References</b>	<b>41</b>

# **Chapter 1- Introduction**

## **1.1 Introduction to Interoception**

Interoception is a term used to describe the brain's ability to sense, process, and interpret bodily signals originating within the body, which are integral for physiological regulation and self-awareness. These internal signals originate from various body systems, including cardiovascular, respiratory, gastrointestinal, genitourinary, nervous, and endocrine systems (Nayok et al., 2023; Tsakiris & Critchley, 2016). It includes a range of sensations such as pain, temperature, itch, tickle, sensual touch, muscle tension, air hunger, stomach discomfort related to low pH, and intestinal tension, which contribute to our integrated perception of the body's physiological state (Craig, 2002). Given the complexity of integrating all these signals, interoception is considered a multi-dimensional construct, involving neurophysiological, neuroanatomical, cognitive, emotional, and behavioral domains (Garfinkel & Critchley, 2017). The importance of sensing internal signals lies in the need to regulate them, thus enabling the body to maintain homeostasis (stability) and allostasis (adaptive change), and facilitating adaptive responses to changing external and internal environments (Fittipaldi et al., 2020).

## **1.2 Neural Pathways of Interoceptive Processing**

Neurophysiologically, interoceptive processing begins with peripheral receptors such as chemoreceptors, mechanoreceptors, and thermoreceptors. Internal signals ascend mainly through two routes. The cranial route transmits visceral information via the vagus and glossopharyngeal nerves to the nucleus tractus solitarius (NTS) in the brainstem (Figure 1). From there, projections continue to the parabrachial nucleus (PBN) and thalamus, and then reach higher-order cortical areas, including the insula, anterior cingulate cortex (ACC), hypothalamus, and amygdala (Figure 2). These regions play complementary roles: the insula supports visceral representation and interoceptive awareness, the ACC contributes to salience and affective evaluation, while the hypothalamus and amygdala regulate homeostatic and emotional responses (Khalsa et al., 2018; Engelen et al., 2023).

The spinal route carries signals from mechanoreceptors sensitive to pressure, stretch, and distension through the splanchnic, phrenic, and cardiac nerves. These afferents ascend via the spinal cord to the NTS and follow the same ascending trajectory through the PBN and thalamus

toward cortical targets (Figure 1). In this way, both cranial and spinal inputs converge on a common brainstem relay before reaching cortical networks that integrate visceral states with emotional and cognitive processes (Craig, 2008).

Three rhythmic physiological signals are especially central to this system: cardiac, respiratory, and gastric rhythms. Coupling is a term used to describe statistical dependence between two signals; here, it is signals between these rhythms and the corresponding neural activity. Respiration is measured with a pneumobelt that detects thoracic or abdominal expansion, or with nasal airflow using spirometry or capnography. Gastric rhythms are recorded with electrogastrography (EGG), where cutaneous electrodes placed over the epigastrium capture slow-wave activity. Finally, cardiac signals are measured with electrocardiography (ECG), which records the heart's electrical activity generated by depolarization and repolarization of the myocardium. The R-wave of the QRS complex provides a precise temporal marker of each heartbeat, making ECG the gold standard for tracking cardiac rhythm. Because this cardiac electrical activity also propagates to the scalp as small field artifacts, it can be detected in EEG recordings and used to align neural responses to each heartbeat (Engelen et al., 2023).

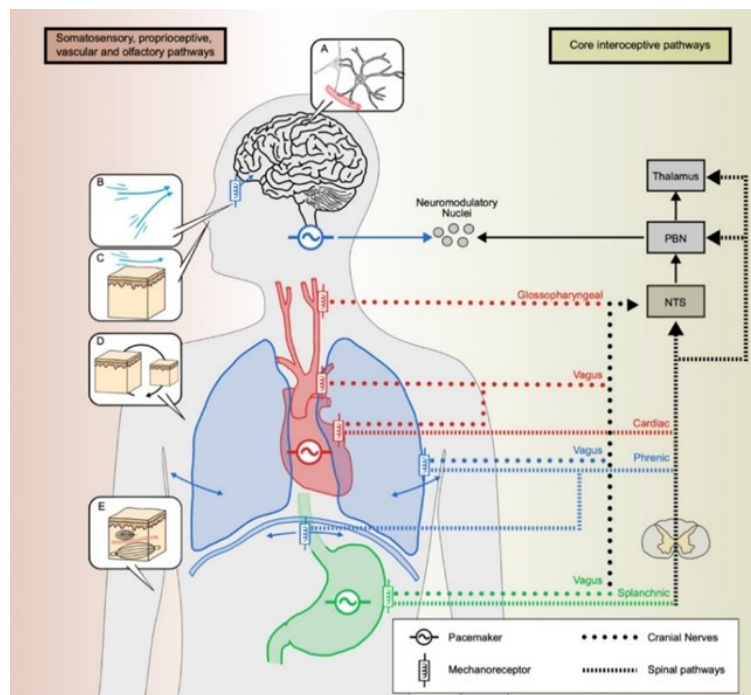


**Figure 1** Illustrated representation of peripheral pathways of interoception. Heartbeat (red), breathing (blue), and stomach rhythms (green) are sensed by mechanoreceptors and travel mainly through the vagus, glossopharyngeal, phrenic, and splanchnic nerves. These signals join in the brainstem at the nucleus tractus solitarius (NTS) and then project via the parabrachial nucleus (PBN) and thalamus to higher cortical areas such as the insula, cingulate, and prefrontal

cortex. Additional somatosensory and olfactory inputs also contribute. Figure adapted from Engelen et al. (2023).

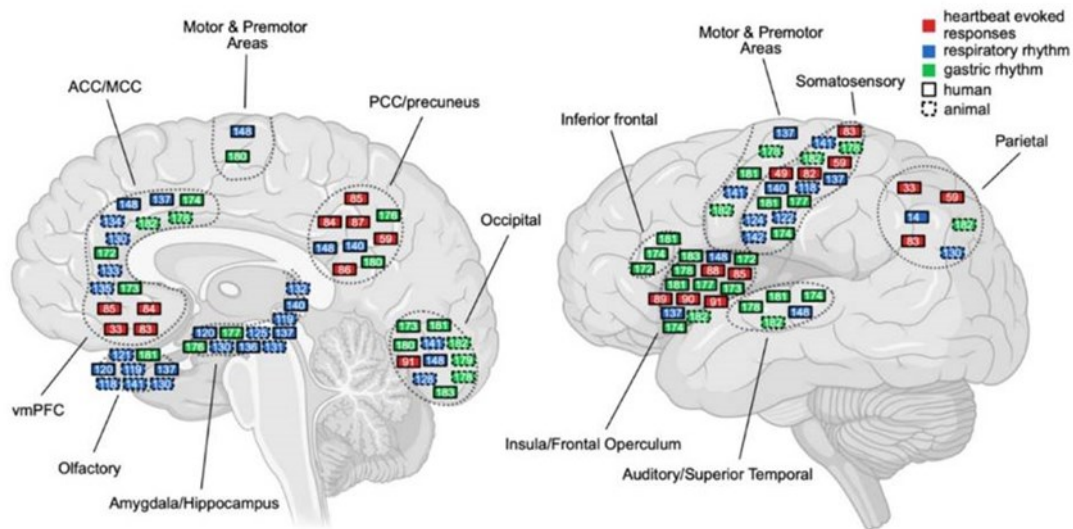


**Figure 2** Brain areas that respond to internal bodily signals are shown for humans (solid outlines) and animals (dashed outlines). Colored boxes indicate the type of signal: red =cardiac rhythm, blue = respiratory rhythm, green = gastric rhythm. Regions include the prefrontal cortex (vmPFC), cingulate cortex (ACC/MCC), insula, somatosensory and motor areas, parietal and occipital cortices, as well as limbic structures (amygdala/hippocampus, olfactory areas). Figure adapted from Engelen et al. (2023).

### 1.3 Cardiac Interoception

Cardiac interoception involves the brain's ability to perceive and process signals from the heart, which are the heartbeat and blood pressure, leading to the maintenance of homeostatic regulation. Moreover, it involves higher-order processes that include emotion, perception, and self-awareness. The focus is on the main organ in cardiac interoception, which is the heart; it has its autonomic pacemaker producing the cardiac cycle. The cardiac cycle consists of i) systole, the heart's contraction phase, the moment when the heart pumps blood into the arteries, which will lead to other body parts, with a fixed duration phase, and ii) diastole, the relaxation phase of the heart where the heart is filled with blood, for which duration is variable. During systole, baroreceptors located in the carotid sinus, aortic arch, heart, and pulmonary vessels detect pressure changes. After the detection signal is relayed via cranial nerves (vagus,

glossopharyngeal) and spinal nerves (cardiac afferents) to NTS and PBN, which are part of brainstem nuclei. Baroreceptors are not the only receptors related to cardiac interoception. Proprioceptive receptors are responsible for detecting blood vessel pulsatility. Astrocytes may also act as intracerebral baroreceptors that modulate brainstem and cortical neurons. Last but not least, PIEZO2 mechanosensitive channels in pyramidal neurons may detect pulse-related membrane tension (Engelen et al. 2023).

#### **1.4 Heart Evoked Potential (HEPs)**

Heart-evoked responses (HERs) describe neural activity related to the heartbeat measured with EEG, fMRI, or MEG (Engelen et al., 2023). Within this, heart-evoked potentials (HEPs) are EEG-based measures time-locked to the R-peak of the ECG, reflecting cortical processing of cardiac signals. The R-peak serves as a trigger to segment EEG into short epochs, and averaging across many trials cancels unrelated activity to reveal the heartbeat-locked response (Al et al., 2020).

Processing steps include R-peak detection (ECG), epoching (−200 - 700 ms), baseline correction (HEP amplitude), and averaging (Figure 3). HEP morphology varies but typically shows an early component (~150 - 250 ms post-R) and a late component (~300 - 400 ms post-R) over fronto-central/centro-parietal scalp (Park & Blanke, 2019). As HEPs are sensitive markers of heartbeat-perception accuracy, studies ask whether individuals differ in HEPs and which conditions drive these differences; analyses typically target early and late post-R-peak windows. Early activity reflects bottom-up registration of cardiac afferents in the posterior insula and somatosensory regions (fronto-central), indexing automatic sensory processing and basic interoceptive awareness (detection that a signal occurred) (Fló et al., 2024); individuals with higher interoceptive accuracy show increased early HEP amplitude. Late activity is more top-down (anterior insula, ACC, prefrontal), reflecting cognitive-affective evaluation and modulation by attention, emotional state, and self-reported processing (Zaccaro et al., 2024); larger late amplitudes appear when attention is directed to heartbeats rather than an external task (Park & Blanke, 2019). Overall, both HEP amplitudes are increased in individuals with higher interoceptive abilities. The early HEP (150 - 250 ms) tracks sensory accuracy, while the late HEP (300 - 500 ms) is especially sensitive to attentional modulation.

Individuals with psychopathological disorders often show reduced interoceptive capacity and poorer awareness of feelings. Disorders marked by emotional dysregulation, such as depression and anxiety, are linked to abnormal HEP modulation (Park & Blanke, 2019). In Generalized

Anxiety Disorder, higher early HEP amplitudes (~240 - 312 ms) have been observed during rest (Verdonk et al., 2023), while social anxiety shows a similar increase (~223 - 305 ms) at Fz during false heartbeat-acceleration cues. In contrast, depression is associated with reduced amplitudes across early and late windows (128 - 264 ms, 356 - 456 ms, 536 - 592 ms) (Flasbeck et al., 2020). To conclude, stronger early responses mark anxiety, while depression shows reduced amplitudes across both early and late windows. Since both disorders involve difficulties in processing and regulating emotions, these HEP changes may point to a broader vulnerability in emotional regulation. This makes emotional dysregulation not a separate outcome, but rather the dimension that should be studied with interoception.

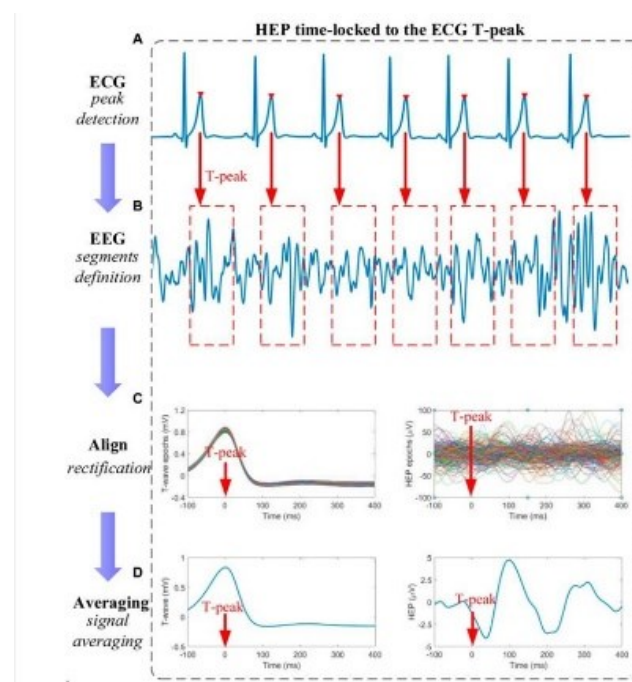


**Figure 3** Illustration of heartbeat-evoked potential (HEP) processing aligned to the ECG T-peak. It is used as an example because the steps are the same for R and T-peak. (A) ECG is recorded, and T-peaks are detected (red arrows). (B) EEG is segmented into epochs around each T-peak. (C) Epochs are aligned to the T-peak to account for variability in cardiac cycle length. (D) Averaging across trials enhances the consistent EEG response time-locked to the heartbeat. Although most HEP studies time-lock to the ECG R-peak, aligning to the T-peak provides an alternative reference that reduces contamination from the QRS complex. Figure adapted from Liu et al. (2023) article.

## 1.5 Altered Interoception and Emotional Dysregulation

William James proposed that “emotion is the feeling of bodily changes”, emphasizing that interoceptive processing, particularly cardiac signals, has been associated with the emotional process, highlighting the role of interoceptive processing in shaping affective states. (Park & Blanke, 2019). Interoceptive processing, when impaired, is characterized by inaccurate perception of internal bodily states. (Paulus & Stein, 2010). These states, according to James, are emotions, and there is evidence that impaired interoception is connected with emotional dysregulation. Emotional dysregulation presents difficulties in identifying, evaluating, controlling, and modulating emotional and behavioral responses.

According to the ability model, emotional dysregulation has six main domains that are: emotional awareness, emotional clarity, nonacceptance of emotional responses, difficulties engaging in goal-directed behavior, impulse control difficulties, and limited access to emotion regulation strategies. These domains can be linked to bad overall mental health, including a higher risk for self-harm and reduced quality of life (Dieujuste et al., 2025).

Neurophysiologically, emotional dysregulation involves dysfunctional interactions within neural circuits, including the insular cortex, ACC, and amygdala, regions critically implicated in emotional and interoceptive integration (Schulz & Vögele, 2015; Owens et al., 2018). Moreover, impaired interoception may contribute significantly to the etiology and progression of various psychiatric disorders marked by emotional dysregulation, such as anxiety, depression, and borderline personality disorder (Khalsa et al., 2018). The study done by Dieujuste et al. (2025) showed that there is interrelatedness between post-traumatic stress disorder (PTSD) and emotional dysregulation, suggesting that emotional dysregulation plays a key role in PTSD. A disorder that is a part category of anxiety disorders, where intense emotions become difficult to manage and contribute to the persistence of symptoms. These findings support the idea that emotion dysregulation is a relevant transdiagnostic factor for understanding and addressing anxiety-related conditions (Dieujuste et al., 2025).

## 1.6 Interoception, Emotion, and Trait Anxiety

Emotional regulation capacities are considered a central issue in how anxiety and depression are maintained and manifest (Barnes et al., 2025).

Chan et al. (2023) investigated how emotion dysregulation (ED) relates to anxiety and depression symptoms in early adolescents, focusing on the role of parent-child attachment. The results show that ED was strongly linked with anxiety and depression and that parent-child attachment can increase vulnerability when ED is present.

Herber et al. (2025) studied how stress, emotion dysregulation, and sleep relate to anxiety and depression in adolescents and young adults. HR, HRV, and subjective stress were measured before, during, and after stress induction. HR normally rises during stress as part of the sympathetic response and then returns to baseline, while HRV decreases due to reduced parasympathetic activity. Results showed that delayed HR recovery to baseline and reduced HRV, together with greater emotion dysregulation, predicted higher anxiety and depression. ED was the strongest predictor of trait anxiety, supporting its role as a transdiagnostic factor in adolescence, a key period for internalizing problems.

Another study showed that ED is a key factor for anxiety vulnerability during adolescence and young adulthood, and it also examined gender differences. Gender was found to moderate this link. Girls reported more anxiety than boys and greater problems with emotional clarity, acceptance, and regulation strategies, which are factors that predicted anxiety mainly in females. Similar patterns are seen in adult neurodivergent groups, where women with autism or intellectual disabilities show higher vulnerability to maladaptive emotional patterns and anxiety (Sáez-Suanes et al., 2022).

In conclusion, ED is strongly linked to anxiety, with interoceptive and physiological processes shaping this connection. Chan et al. (2023) showed that this link is bidirectional in adolescence and influenced by parent-child attachment. Herber et al. (2025) found that poor regulation appears in slower heart rate baseline recovery and reduced HRV after stress, predicting greater anxiety. Bender et al. (2012) highlighted gender risks, with girls reporting more anxiety and difficulties in clarity, acceptance, and regulation strategies, while Sáez-Suanes et al. (2023) showed that women with autism are especially vulnerable. Together, these studies show that problems in emotion regulation and altered interoception contribute to anxiety, with women particularly at risk.

## 1.7 Interoception, Emotion, and Impulsivity

Impulsivity has been defined as a predisposition for rapid, unplanned actions in response to external and internal stimuli without considering the negative consequences of these actions. It has been associated with quick decision-making and a lack of planning. Even if it is a normal personality trait, it's often considered maladaptive, varying across individuals. (Baiano et al., 2021).

In a systematic review, Bruton et al. (2024) investigated the relationship between interoception and ADHD symptoms, including impulsivity, emotional dysregulation, and executive dysfunction, in both clinical and non-clinical populations. They found that individuals with more severe ADHD symptoms, including impulsivity, have lower interoception.

Herman (2023) reviewed the interoceptive inference framework, which states that the brain continuously predicts internal bodily states to maintain homeostasis. When these predictions are inaccurate, often due to poor interoception, individuals may experience undifferentiated arousal and engage in impulsive behaviors as maladaptive coping strategies.

Hebb (1955) proposed that everyone has an optimal level of arousal, defined as cortical excitation and autonomic activation. Individuals with chronically low arousal may engage in impulsive behaviours to increase stimulation and restore homeostasis. This theory has been extended to personality models, suggesting that impulsive individuals are highly sensitive to reward signals and are prone to raising their arousal levels through different behaviours (Herman et al., 2019).

Jenkinson et al. (2024) demonstrated that individuals with high impulsivity and low interoceptive accuracy showed higher activation of the amygdala during uncertain decision-making, suggesting a poor relation between emotions and the body.

In a study, Carlson & Thái (2010) found that late P3 (300 - 600 ms) amplitude is associated with traits related to impulsivity and antisocial behavior. This suggests that higher impulsivity may be linked to decreased P3 amplitude.

Together, these results suggest that impulsivity is closely related to impaired interoception in both clinical and non-clinical samples and that there is a possible different correlation between impulsivity and early and late HEP amplitudes.

## **1.8 Interoception, Emotion, and Affective Lability**

Affective lability is a rapid shift in outward emotional expressions and is one aspect of affect dysregulation and is closely linked to dysregulated interoception. Affective lability is a primary feature of many psychological disorders, including depression, bipolar disorder, borderline personality disorder, and intermittent explosive disorder (Look et al., 2010). Studies showed that individuals with high affective lability often present lower HRV and neural responses to cardiac signals, pointing to difficulties in linking bodily signals with emotional processing.

In the study by Flasbeck et al. (2020), individuals with borderline personality disorder had higher HEP amplitude over frontal electrodes. Three-time windows were taken into account: 250 - 450 ms (early), 455 - 595 ms (late-1), and 524 - 620 ms (late-2), with window-specific alterations and maximal effects in the 455 - 595 ms range (Flasbeck et al., 2020). Another study found reduced HEP amplitude across early and late windows in patients with depression, implying altered interoception and emotional sensitivity in this group (Terhaar et al., 2012).

These findings suggest that affective lability in the clinical population is marked by impaired interoceptive processes that fail to provide a basis for emotional regulation across different disorders.

## **1.9 Sex Differences in Interoception and Emotional Reactivity**

Significant sex differences have been observed in both interoception and emotional regulation. Women tend to perform lower on cardiac interoception tasks but report higher subjective awareness and sensitivity to internal bodily states (Tummeltshammer et al., 2019). This increased interoceptive sensitivity is often associated with increased emotional reactivity and a higher likelihood of emotional dysregulation. Neuroimaging evidence further reveals that women show stronger cortical activation in the prefrontal cortex and insula during emotional processing, implying compensatory mechanisms to manage increased emotional salience (Min et al., 2023). These combined insights strongly support the relevance of studying emotion regulation and interoception in women.

To sum up, all these suggest that increased interoceptive sensitivity, combined with stronger emotional reactivity, are vulnerability factors that make women more prone to emotion dysregulation.

## 1.10 Aims and hypotheses

To test whether heartbeat-evoked potentials (HEPs) differ between women with high vs. low emotion dysregulation (ED) at rest, and how early (N1, 150 - 250 ms) and late (P1, 300 - 400 ms) HEP amplitudes relate to trait anxiety, impulsivity, and affective lability.

H1: We expect in relation to the low-dysregulation (LD) group, that the high-dysregulation (HD) group will show larger N1 amplitudes (150 - 250 ms) and smaller P1 amplitudes (300 - 400 ms) over centro-parietal sites, consistent with heightened bottom-up sensitivity and reduced late evaluative control of interoceptive signals (Flasbeck et al., 2020; Park & Blanke, 2019).

H2: Within the HD group, higher anxiety (STAI-T), impulsivity (UPPS-P), and affective lability (ALS-18) will correlate positively with N1 amplitude and negatively with P1 amplitude. In the LD group, these associations will be weak or non-significant.

## **Chapter 2 - Materials and Methods**

### **2.1 Participants and Data**

The data used in this study were originally collected for a research project resulting in the scientific publication Fusina et al. (2022), which was oriented to the investigation of neurophysiological correlates of emotion dysregulation in a non-clinical female population. From a sample that involved 422 female university students, 25 with high emotional dysregulation (HD) and 25 with low emotional dysregulation (LD) were selected, for EEG recording during a five-minute resting state with eyes open.

The present study aims to conduct a secondary analysis of these data, focusing on the investigation of HEPs, heart rate variability (HRV), and individual differences in psychological traits such as anxiety, affective lability, and impulsivity in high and low emotionally dysregulated groups. Also, the relationships between these measurements were explored.

For this study, a sample of 43 female participants was used. In the first low emotionally dysregulated group, there were 20 participants, and in the high emotionally dysregulated group, there were 23 female participants. From the sample of 50 female participants from Fusina et al.'s (2022) study, 7 participants were excluded due to poor ECG data quality. The combination of EEG/ECG physiological recordings with these self-report measures offers a multimodal framework to investigate how alterations in interoceptive processing may underlie emotional and behavioral dysregulation in a non-clinical female population.

### **2.2 Psychometric Measures**

To investigate the relationship between neural indices and individual psychological characteristics, participants completed three psychometrically validated questionnaires (Fusina et al., 2022):

The State-Trait Anxiety Inventory - Trait (STAI-T) (Spielberger, 1983) was used to assess stable dispositional anxiety. It includes 20 self-report items rated on a 4-point Likert scale ranging from “Almost Never” to “Almost Always.” Higher scores indicate greater levels of trait anxiety.

The UPPS-P Impulsive Behavior Scale (Whiteside & Lynam, 2001; Cyders & Smith, 2007) is a multidimensional measure that captures five distinct facets of impulsivity: Negative Urgency,

Positive Urgency, (lack of) Premeditation, (lack of) Perseverance, and Sensation Seeking. The short version used in this study consisted of 20 items, a 4-point Likert scale (1 = strongly agree; 4 = strongly disagree). Subscale scores and a global impulsivity score were computed.

The Affective Lability (ALS-18) was used to assess affective lability or the tendency for rapid, marked shifts in mood. The ALS-18 (0–3 Likert scale, higher = more lability) yields three subscales, Depression/Elation, Anxiety/Depression, and Anger, with higher scores indicating greater lability. It is the validated 18-item short form of the original Affective Lability Scales and has an Italian validation with a comparable three-factor structure (Owens et al., 2018).

Lower resting HRV has been associated with greater affective instability in daily life, supporting exploratory links between ALS-18 and HRV/HEP in emotion dysregulation samples. Cardiac interoception and autonomic control are also interrelated, where HR and HRV reflect the autonomic nervous system regulation of bodily arousal, and HEPs capture cortical processing of cardiac signals. Together, they represent different levels of the same brain–body regulatory system. Autonomic flexibility, reflected in HRV, provides the physiological basis for emotional stability, while cortical processing of cardiac signals, reflected in HEPs, contributes to the conscious experience of these bodily states. This interdependence provides logical motivation to examine HRV and HEP in parallel with self-report traits, reflecting emotional dysregulation in our sample. (Koval et al. 2013).

### **2.3 Physiological measurements**

In the Fusina et al. (2022) study, before the EEG recording, the Affective Lability Scales-18 (ALS-18) questionnaire was re-administered to participants. This step was crucial to ensure the correct attribution of subjects to either the high dysregulation (HD) or low dysregulation (LD) groups, as the ALS-18 was the most represented questionnaire in the Principal Component Analysis (PCA) loadings used for group formation. A 64-channel EEG elastic cap (ElectroCap) was used, fitted with 57 scalp electrodes and 7 external electrodes. These external electrodes included those placed on the nasion, external canthi, and mastoids. Participants were asked to sit back, relax with their eyes open, and look in front of them for 5 minutes each. Data were recorded using a SynAmps amplifier at a 500 Hz sampling rate, with a bandwidth set from 0 to 100 Hz, and EEG channels were online referred to the Cz electrode.

### 2.3.1 EEG/ECG Pre-processing

EEG pre-processing was performed by Fusina et al. (2022) by using the Noninvasive Electrophysiology Toolbox (NET; Taberna et al., 2024), which offers an automated pipeline, based on MATLAB, to perform advanced EEG data analyses. The pre-processing included bad channel detection that was identified based on two parameters: i) minimum Pearson correlation between each channel signal and all other channels within a 1-50 Hz frequency range, and ii) noise variance in the 200-250Hz frequency range. Channels exceeding 3 standard deviations above the mean of either parameter were classified as bad and subsequently interpolated using the FieldTrip toolbox. Data were then band-pass filtered between 1–50 Hz using EEGLAB. Artifacts related to eye movements and muscle activity were removed by applying a fast fixed-point ICA (FastICA) algorithm. Independent components were automatically rejected based on three metrics: (i) correlation of IC power with vertical and horizontal EOG and EMG signals, (ii) deviation of the IC power spectrum from a 1/f function, and (iii) kurtosis of the IC time course. Finally, source localization was conducted using the standardized low-resolution brain electromagnetic tomography (sLORETA) algorithm, implemented on a 6 mm homogeneous grid. A standard head model was constructed from a template MRI combined with manufacturer-provided template electrode positions for the purpose of their study. In the present re-analysis, we did not perform source localization; all statistics were at the sensor level.

### 2.3.2 EEG/ECG Processing

For heartbeat alignment, R-peaks were detected in the ECG channel using a method adapted from Marino et al. (2018). The Adaptive Optimal Basis Set (aOBS) algorithm was originally developed to identify and remove ballistocardiographic (BCG) artifacts in EEG recorded simultaneously with fMRI, a procedure that requires precise detection of R-peaks in the ECG signal. In the present study, the same principle was repurposed to obtain robust R-peak detection in our EEG recordings. This method accounts for variability in the delay between cardiac and EEG activity, providing more reliable detection than simple thresholding. The ECG was band-pass filtered (5–20 Hz), squared, and smoothed with a 0.1–2 Hz envelope. Peaks were detected using an adaptive threshold ( $5\times$  the ECG SD) with a minimum peak distance of 0.3 s (Poppa et al., 2022). After detecting R-peaks, EEG data were segmented into epochs time-locked to these events (–200 to 700 ms; 485 samples at 500 Hz). In this study, NET was also

used for epoching, baseline correction, averaging, and scalp current density (Laplacian) transformation. To improve data quality, the EEG was filtered from 1–50 Hz, baseline-corrected using the –200 to –50 ms pre-R-peak interval, and screened for artifacts. Epochs exceeding  $\pm 50 \mu\text{V}$  on any channel were rejected. On average, 484 epochs per subject (SD = 4.95, range = 450–485) were retained after artifact rejection and baseline correction. Finally, waveforms were transformed to scalp current density ( $\mu\text{V}/\text{cm}^2$ ) with FieldTrip’s spline method, a step that enhances spatial specificity by reducing volume conduction.

## 2.4 Statistical Analysis

All statistical analyses were performed in MATLAB and FieldTrip. Group differences between high and low dysregulation participants were first assessed at the sensor level using independent-samples t-tests and non-parametric rank-sum tests on HEP amplitudes, computed point-by-point across channels and time samples.

To obtain subject-level summary metrics, Global Field Power (GFP) was computed as the standard deviation across channels at each time point. GFP represents the overall strength of neural activity at each time point, calculated as the standard deviation across all electrodes, providing a reference-free and channel-independent measure. Group mean GFP traces were compared using independent-samples t-tests. For region-of-interest analyses, mean amplitude, peak amplitude, and peak latency were extracted for each subject within predefined early (150 - 250 ms) and late (300 - 400 ms) HEP windows over CP1.

Associations between HEP features and psychological measures (STAI-T, UPPS-P, ALS-18) were examined separately within each group using Spearman’s rank correlations ( $\rho$ ). Significance was set at  $p < 0.05$ .

## Chapter 3 - Results

### 3.1 Questionnaires

#### 3.1.1 Group differences

Group differences in questionnaire scores were examined, see differences between high (HD) and low (LD) dysregulation groups. Participants in the HD group scored significantly higher on the ALS-18 total scale (mean = 35.84, SD = 6.76) compared to the LD group (mean = 7.96, SD = 5.16),  $t = 16.40$ ,  $p < 0.001$ ). Similarly, the HD group reported greater levels of trait anxiety on the STAI (mean = 56.40, SD = 8.09) than the LD group (mean = 37.16, SD = 6.06),  $t = 9.51$ ,  $p < 0.001$ . Finally, impulsivity, as measured by the UPPS-P, was also significantly higher in the HD group (mean = 148.32, SD = 24.61) compared to the LD group (mean = 114.92, SD = 13.12),  $t = 5.99$ ,  $p < 0.001$ ) (Table 1). These findings confirm that the two groups differed robustly on trait anxiety, affect lability, and impulsivity, supporting the group selection criteria and providing a strong basis for subsequent physiological analyses.

Questionnaire	HD (mean $\pm$ SD)	LD (mean $\pm$ SD)	t	p
ALS-18	35.84 $\pm$ 6.76	7.96 $\pm$ 5.16	16.4	< 0.001*
STAI-Trait	56.4 $\pm$ 8.09	37.16 $\pm$ 6.06	9.51	< 0.001*
UPPS-P	148.32 $\pm$ 24.61	114.92 $\pm$ 13.12	5.99	< 0.001*

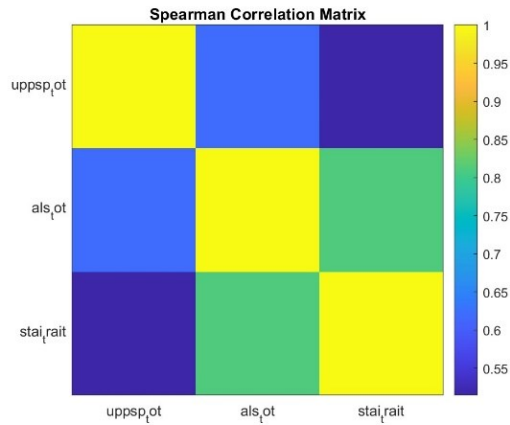
**Table 1** Group differences in questionnaire scores between high (HD) and low (LD) emotional dysregulation participants. Mean  $\pm$  SD values are shown for each measure, along with  $t$ -statistics and  $p$ -values from independent-samples  $t$ -tests.

### 3.1.2 Correlations between questionnaires

The correlations between questionnaires were computed to investigate how the three self-report measures relate to one another. We computed Spearman's rho ( $\rho$ ) correlations across all participants (Table 2). ALS-18 scores were strongly correlated with both UPPS-P ( $\rho = 0.64$ ,  $p < 0.001$ ) and STAI-Trait ( $\rho = 0.84$ ,  $p < 0.001$ ), indicating that individuals with higher affective lability also tended to report greater impulsivity and anxiety. UPPS-P and STAI-Trait were also moderately correlated ( $\rho = 0.58$ ,  $p < 0.001$ ). Taken together, these results suggest that while the constructs are interrelated, each captures unique aspects of emotional dysregulation.

	<b>UPPS-P</b>	<b>ALS-18</b>	<b>STAI-Trait</b>
<b>UPPS-P</b>	$\rho = 1.00$	$\rho = 0.64$	$\rho = 0.58$
	$p = 1.00$	$p < 0.001^*$	$p < 0.001^*$
<b>ALS-18</b>	$\rho = 0.64$	$\rho = 1.00$	$\rho = 0.84$
	$p < 0.001^*$	$p = 1.00$	$p < 0.001^*$
<b>STAI-Trait</b>	$\rho = 0.58$	$\rho = 0.84$	$\rho = 1.00$
	$p < 0.001^*$	$p < 0.001^*$	$p = 1.00$

**Table 2** Spearman's Correlations Between Questionnaire Scores (N = 43). Values are Spearman's correlation coefficients ( $\rho$ ).  $**p < 0.001$ .



**Matrix 1** Spearman correlation matrix for UPPS-P, ALS-18, and STAI-Trait scores. Brighter colors indicate stronger positive correlations, with values ranging from 0.55 (dark blue) to 1.00 (yellow). All correlations were significant at  $**p < 0.001$ .

### 3.2 HEP results

#### 3.2.1 Grand average and Global Field Power (GFP)

Grand-average HEP waveforms were computed across all participants and plotted for each electrode as shown in Figure 4, without separating into groups, from -200 ms to 700 ms time window. Two clear components can be observed: an early component, N1 (~150 - 250 ms), and a late component, P1 (~300 - 400 ms).

The grand average waveform across 57 EEG channels for two groups (LD and HD) was performed (Figures 5 and 6). Each line represents the average waveform of one electrode, time-locked to the ECG R-peak (0 ms). Both groups display an early component (~150 - 250 ms) and a late component (~300 - 400 ms).

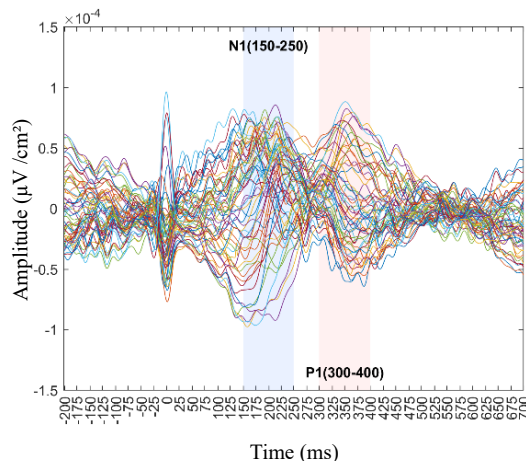


**Figure 4** Grand average HEP waveform across all 57 EEG channels and all participants. Each colored line represents the average HEP waveform from one electrode, time-locked to the ECG R-peak (0 ms). Data are averaged across all participants and displayed from  $-200$  to  $700$  ms. Two main components are visible: an early component (N1;  $\sim 150 - 250$  ms) and a late component (P1;  $\sim 300 - 400$  ms).

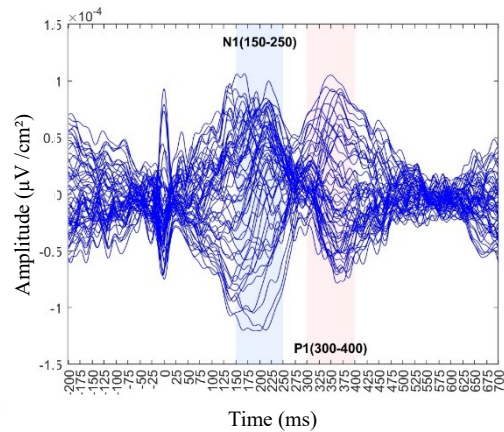


**Figure 5** Grand average HEP waveforms for the LD group. Grand average waveforms across 57 EEG channels for the low dysregulation group, time-locked to the ECG R-peak (0 ms). Data are shown from  $-200$  to  $700$  ms. An early ( $\sim 150 - 250$  ms) and a late ( $\sim 300 - 400$  ms) component are visible.

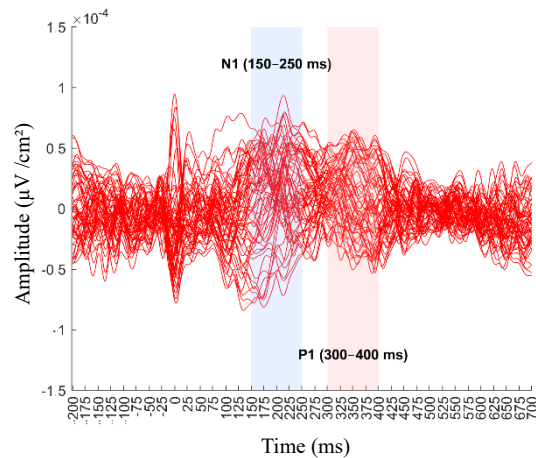


**Figure 6** Grand average HEP waveforms for the HD group. Grand average waveforms across 57 EEG channels for the high dysregulation group, time-locked to the ECG R-peak (0 ms). Data are shown from  $-200$  to  $700$  ms. An early ( $\sim 150 - 250$  ms) and a late ( $\sim 300 - 400$  ms) component are visible.

To further investigate group-level differences, global field power (GFP) was computed for low emotionally dysregulated (LD; Figure 7) and high emotionally dysregulated (HD; Figure 8) groups. A point-by-point *t*-test on GFP identified a significant difference in the 325–450 ms window (Figure 9). From this analysis, a significant group difference was revealed during the P1 late component (325 - 450 ms). The LD group showed higher GFP amplitude compared to the HD group (Figure 9). These results indicate that women with lower emotional dysregulation have stronger or more widespread cortical responses to cardiac signals during the late stages of interoceptive processing compared to those with high emotional dysregulation.

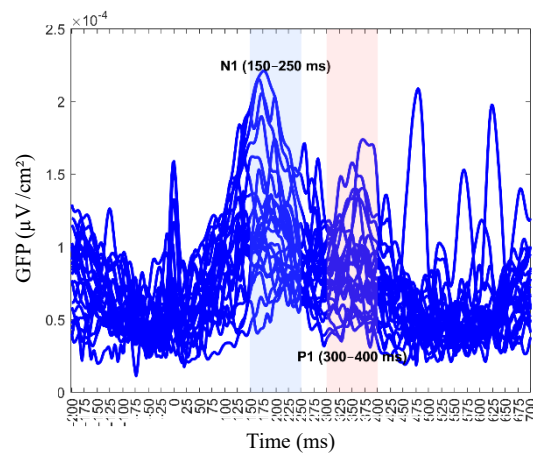


**Figure 7** The GFP waveform represents the overall strength of neural activity across 57 EEG channels, computed as the standard deviation of voltage values at each time point relative to the ECG R-peak (0 ms). Data are averaged across participants in the LD group and plotted from –200 to 700 ms.

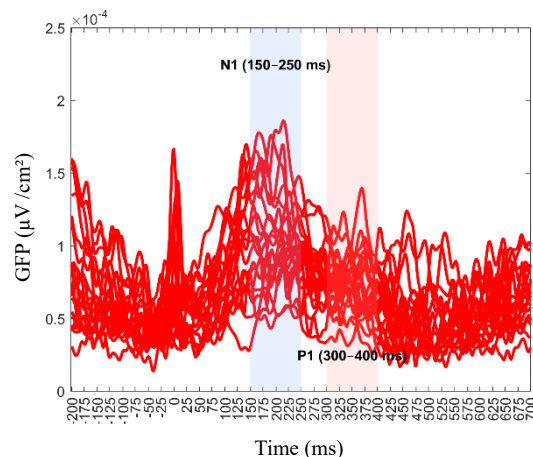


**Figure 8** GFP of the HD group. The GFP waveform represents the overall strength of neural activity across 57 EEG channels, computed as the standard deviation of voltage values at each time point relative to the ECG R-peak (0 ms). Data are averaged across participants in the HD group and plotted from –200 to 700 ms.

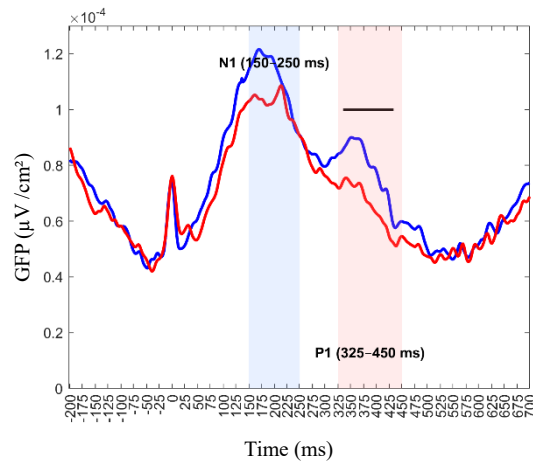


**Figure 9** Comparison of GFP between high and low dysregulation groups. Global Field Power (GFP) waveforms for the low dysregulation (LD, blue) and high dysregulation (HD, red) groups are shown from  $-200$  to  $700$  ms relative to the ECG R-peak ( $0$  ms). GFP reflects the standard deviation of voltages across all  $57$  EEG channels at each time point, providing a channel-independent measure of neural response strength. The black horizontal bar indicates the time window ( $325 - 450$  ms) where point-by-point t-tests revealed significant group differences, with the LD group showing higher GFP values than the HD group.

### 3.2.2 Topographical Distribution

Time windows of interest were first identified from the grand-average waveforms and GFP curves, which consistently showed an early (N1,  $\sim 150 - 250$  ms) and a late (P1,  $\sim 300 - 400$  ms) deflection. Based on these windows, topographical maps were computed to examine the spatial distribution of HEP activity. Topographical maps were generated for the  $0-400$  ms window in each group (Figures 10 and 11). Both groups displayed centro-parietal distribution, with activity becoming more pronounced in the  $150-250$  ms (N1) and  $300-400$  ms (P1) windows. However, the LD group (Figure 11) exhibited stronger and more spatially extended responses, especially over left centro-parietal electrodes (CP1, CP3, P1, P3, TP7), compared to the HD group (Figure 10).

Following prior research, CP1 (channel 33) was selected as the electrode of interest for further analyses. Zaccaro et al. (2024) reported HEP modulations over centro-parietal sites, including CP1, in both early ( $\sim 170 - 330$  ms) and late ( $\sim 352 - 508$  ms) windows, particularly during interoceptive attention and exhalation. These findings converge with earlier reports of HEP sensitivity at centro-parietal electrodes (e.g., CP1, CPz, P1), supporting the relevance of this

location for capturing interoceptive processing. On this basis, we restricted our analyses to CP1, examining mean amplitudes in early (150–250 ms) and late (300–400 ms) windows.

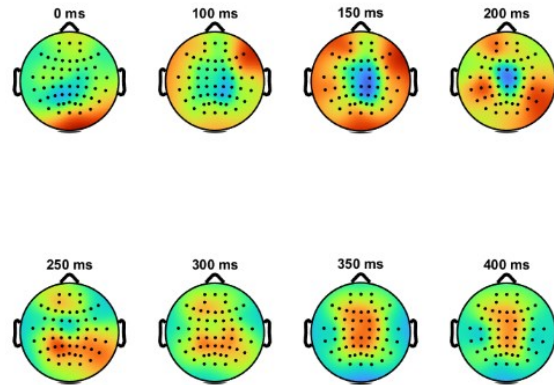


**Figure 10** Topographical distribution of heartbeat-evoked potentials (HEPs) in the high dysregulation (HD) group. The maps show activity at successive time points from 0 - 400 ms relative to the R-peak, with responses observed over centro-parietal regions in the early (150 - 250 ms, N1) and late (300 - 400 ms, P1) windows.

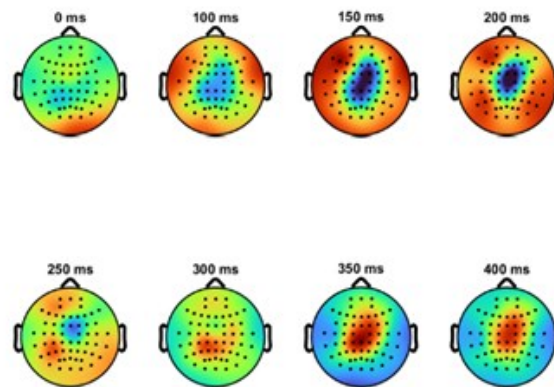


**Figure 11** Topographical distribution of heartbeat-evoked potentials (HEPs) in the low dysregulation (LD) group.

To further illustrate the choice of CP1, grand-average waveforms were plotted for both groups at this electrode (Figure 12). These waveforms clearly showed HEP morphology, with an early

negative deflection (N1; ~150 - 250 ms) followed by a later positive deflection (P1; ~300 - 400 ms), reflecting normal interoception phases. Consistent with the GFP and topographical analyses, the LD group exhibited a stronger late positive component compared to the HD group, while both groups showed a comparable early negativity. Presenting the grand-average waveforms at CP1 highlights the temporal dynamics that guided our selection of this site and windows of interest, providing a reference for subsequent group comparisons and correlation analyses.

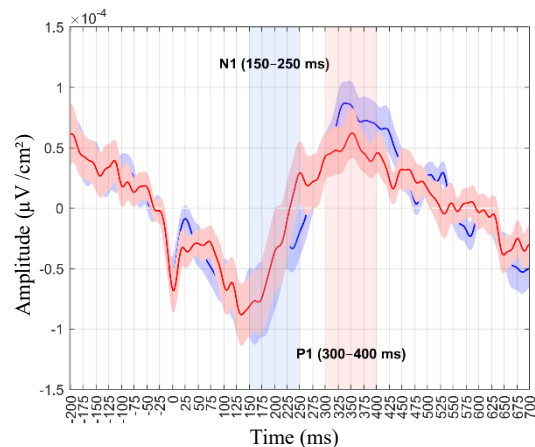


**Figure 12** Grand-average heartbeat-evoked potentials (HEPs) at CP1 for high (HD; red) and low (LD; blue) dysregulation groups. Waveforms are time-locked to the ECG R-peak (0 ms) and displayed from -200 to 700 ms. Shaded regions represent  $\pm 1$  SEM. Both groups show an early negative deflection (N1; ~150 - 250 ms) and a later positive deflection (P1; ~300 - 400 ms).

### 3.3 Cardiac physiology (ECG/HRV)

#### 3.3.1 Descriptives and group differences

Cardiac physiology provides important indices of autonomic nervous system regulation. At rest, heart rate (HR) reflects the overall balance between sympathetic and parasympathetic influences on the sinoatrial node. Beyond mean HR, heart rate variability (HRV) offers a more sensitive measure of autonomic flexibility and emotion regulation capacity. HRV quantifies the beat-to-beat variability of successive R-R intervals in the ECG signal and can be derived through several time-domain parameters.

Among these, SDNN (standard deviation of NN intervals) represents the overall variability of the cardiac cycle, integrating both sympathetic and parasympathetic influences. RMSSD (root

mean square of successive differences) primarily indexes parasympathetic (vagal) activity and is widely used as a marker of flexible emotional and physiological regulation. pNN50 (percentage of successive intervals differing by more than 50 ms) similarly reflects vagal modulation and short-term HRV. Together, these measures capture complementary aspects of cardiac autonomic control, providing insight into physiological mechanisms that may underlie emotional dysregulation. Descriptive statistics for mean HR and HRV indices across the low (LD) and high (HD) dysregulation groups are presented in Table 3.

Group comparisons were conducted using independent-samples *t*-tests when assumptions of normality were met, and Mann–Whitney U tests otherwise. Results showed no significant differences between high and low dysregulation groups in Mean HR, SDNN, RMSSD, or pNN50 (Table 4). This suggests that resting-state autonomic physiology did not robustly distinguish HD from LD participants in this sample.

<b>Measure</b>	<b>LD mean ± SD</b>	<b>HD mean ± SD</b>	<b>Test</b>	<b>p</b>
<b>Mean HR (bpm)</b>	78.49 ± 6.56	82.03 ± 8.63	t = -1.58	0.122
<b>SDNN (ms)</b>	76.52 ± 37.54	90.80 ± 57.94	U = 580	0.877
<b>RMSSD (ms)</b>	65.73 ± 33.76	82.19 ± 59.95	U = 577	0.825
<b>pNN50 (%)</b>	30.79 ± 17.35	34.17 ± 23.96	t = -0.55	0.582

**Table 4** Group Differences in Heart Rate (HR) and HRV Indices Between Low and High Emotional Dysregulation Groups. Note. Values represent group means ± standard deviations (SD). Independent-samples *t*-tests were used when normality assumptions were met (Mean HR, pNN50); Mann–Whitney U tests were applied when distributions deviated from normality (SDNN, RMSSD). HR = heart rate; SDNN = standard deviation of NN intervals; RMSSD = root mean square of successive differences; pNN50 = percentage of successive NN intervals > 50 ms.

### 3.4. Correlational analysis

Beyond group comparisons, we examined whether individual variability in physiological measures was associated with psychological traits. First, we tested correlations between HEP amplitudes and questionnaire scores (ALS-18, UPPS-P, STAI-T). Next, we explored associations between HRV indices and both self-report and neural measures to evaluate potential autonomic–cortical coupling.

#### 3.4.1 HEP and Questionnaires

At the predefined electrode of interest (CP1), Spearman’s rho ( $\rho$ ) correlations were computed between N1 (150–250 ms) and P1 (300–400 ms) amplitudes and questionnaire scores (ALS-18, UPPS-P, STAI-T). Results are summarized in Table 5.

Questionnaires	Group	Amplitude	Spearman’s $\rho$	p
<b>UPPS-P</b>	<b>HD</b>	<b>N1</b>	<b>0.53</b>	<b>0.02*</b>
	<b>HD</b>	<b>P1</b>	<b>-0.47</b>	<b>0.04*</b>
	LD	N1	0.02	0.9
	LD	P1	0.2	0.36
<b>ALS-18</b>	<b>HD</b>	<b>N1</b>	<b>0.52</b>	<b>0.01*</b>
	<b>HD</b>	<b>P1</b>	<b>-0.47</b>	<b>0.03*</b>
	LD	N1	0.02	0.9
	LD	P1	0.2	0.35
<b>STAI-T</b>	<b>HD</b>	<b>N1</b>	<b>0.53</b>	<b>0.01*</b>
	<b>HD</b>	<b>P1</b>	<b>-0.47</b>	<b>0.03*</b>
	LD	N1	0.002	0.98
	LD	P1	0.2	0.26

**Table 5** Correlations Between HEP Amplitudes at CP1 and Self-Reported Questionnaire Scores in High (HD) and Low (LD) Dysregulation Groups. HEP = heartbeat-evoked potential; N1 = 150–250 ms; P1 = 300–400 ms; UPPS-P = Urgency, Premeditation, Perseverance, Sensation Seeking, and Positive Urgency scale; ALS-18 = Affective Lability Scale–18; STAI-T = State–Trait Anxiety Inventory, Trait version. Significant correlations are highlighted in bold.

### 3.4.2 Impulsivity (UPPS-P) and HEP

To examine the relationship with impulsivity, Spearman’s rho ( $\rho$ ) correlations between UPPS-P scores and HEP amplitudes, at the CP1 electrode, were computed separately for each group. In the HD group, significant correlations were found for both HEP components. A positive correlation with N1 ( $\rho = 0.53$ ,  $p = 0.02$ ) and a negative correlation with P1 component ( $\rho = -0.47$ ,  $p = 0.04$ ), as shown in Figures 13 and 14. These results suggest that higher impulsivity in emotionally dysregulated individuals relates to increased early cortical responses (N1), yet diminished later processing (P1). No significant results were found for the LD group.

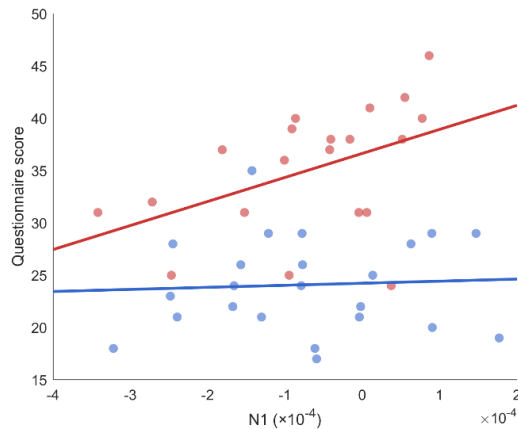


**Figure 13** Correlation between N1 amplitude at CP1 and UPPS-P scores. The red colour represents the HD group, while the blue colour represents the LD group. For the HD group, correlation with N1 amplitude was  $\rho = 0.53$ ,  $p = 0.02^*$ , and for the LD group was  $\rho = 0.002$ ,  $p = 0.9$ . Scatterplots show associations between N1 amplitude (x-axis; in  $\mu\text{V}/\text{cm}^2 \times 10^{-4}$ ) and questionnaire scores (y-axis). Each dot represents one participant (HD = red, LD = blue). Regression lines indicate group-specific trends.

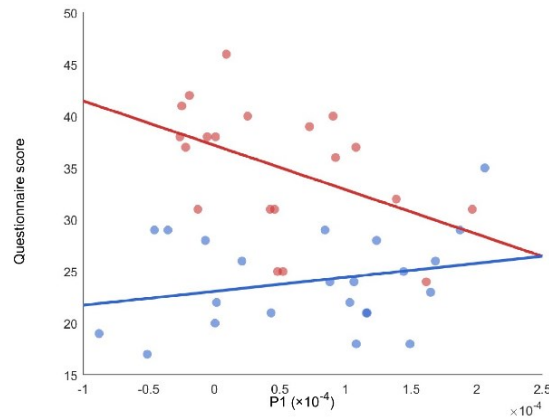


**Figure 14** Correlation between P1 amplitude at CP1 and UPPS-P scores. The red colour represents the HD group, while the blue colour represents the LD group. For the HD group, correlation with P1 amplitude was  $\rho = -0.47$ ,  $p = 0.04^*$ , and for the LD group was  $\rho = 0.2$ ,  $p = 0.36$ . Scatterplots show associations between P1 amplitude (x-axis; in  $\mu\text{V}/\text{cm}^2 \times 10^{-4}$ ) and questionnaire scores (y-axis). Each dot represents one participant (HD = red, LD = blue). Regression lines indicate group-specific trends.

### 3.4.3 Affective Lability (ALS-18) and HEP

Furthermore, the relationship between affective lability and HEP amplitudes was analysed. Within the HD group, affective lability correlated positively with N1 amplitude ( $\rho = 0.53$ ,  $p = 0.01$ ) and significantly negatively with P1 amplitude ( $\rho = -0.47$ ,  $p = 0.03$ ), as illustrated in Figures 15 and 16. No significant correlations appeared in the LD group. These findings suggest that individuals reporting higher affective lability show enhanced early cortical responsiveness followed by weaker late-stage processing of cardiac signals, reflecting potential interoceptive dysregulation in this sample

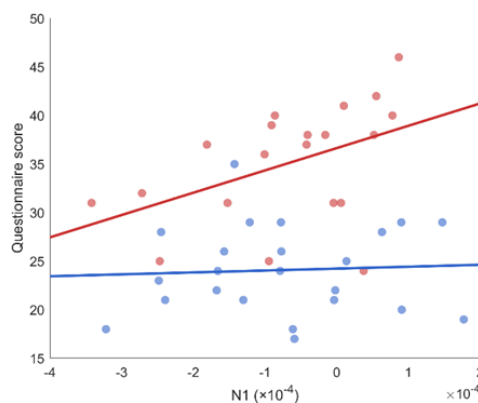


**Figure 15** Correlation between N1 amplitude at CP1 and ALS-18 scores. The red colour represents the HD group, while the blue colour represents the LD group. For the HD group, correlation with N1 amplitude was  $\rho = 0.52$ ,  $p = 0.01^*$ , and for the LD group was  $\rho = 0.02$ ,  $p = 0.9$ .

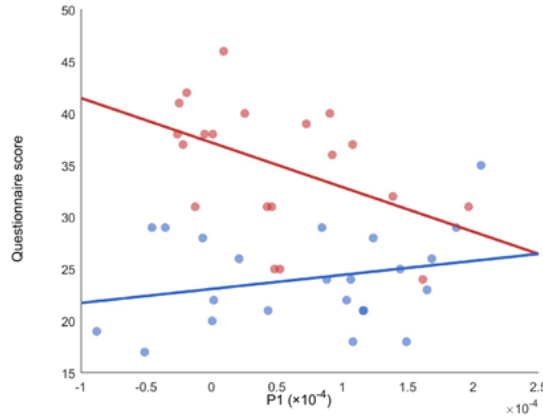


**Figure 16** Correlation between P1 amplitude at CP1 and ALS-18 scores. The red colour represents the HD group, while the blue colour represents the LD group. For the HD group, correlation with P1 amplitude was  $\rho = -0.47$ ,  $p = 0.03^*$ , and for the LD group was  $\rho = 0.2$ ,  $p = 0.35$ .

### 3.4.4 Trait Anxiety (STAI-T) and HEP

Correlations between trait anxiety (STAI-T) and HEP amplitudes at CP1 were then examined. Within the HD group, trait anxiety correlated significantly and positively with N1 amplitude ( $\rho = 0.53$ ,  $p = 0.01$ ) and significantly negatively with P1 amplitude ( $\rho = -0.47$ ,  $p = 0.03$ ), as illustrated in Figures 17 and 18. No significant correlations appeared in the LD group. These findings suggest that in this sample, individuals reporting higher trait anxiety show enhanced early cortical responsiveness followed by weaker late-stage processing of cardiac signals.

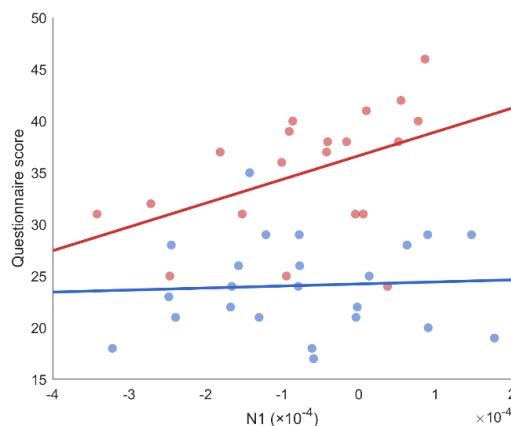


**Figure 17** Correlation between N1 amplitude at CP1 and STAI-T scores. The red colour represents the HD group, while the blue colour represents the LD group. For the HD group, correlation with N1 amplitude was  $\rho = 0.53$ ,  $p = 0.01^*$ , and for the LD group was  $\rho = 0.002$ ,  $p = 0.98$ .

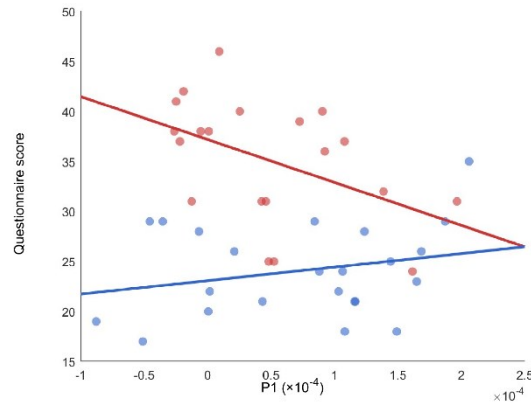


**Figure 18** Correlation between P1 amplitude at CP1 and STAI-T scores. The red colour represents the HD group, while the blue colour represents the LD group. For the HD group, correlation with P1 amplitude was  $\rho = -0.47$ ,  $p = 0.03^*$ , and for the LD group was  $\rho = 0.2$ ,  $p = 0.26$ .

### 3.4.5 HR, HRV, and HEP

To explore the relationship between cardiac autonomic regulation and interoceptive brain responses, we examined Spearman's correlations between HR and HRV metrics (MeanHR, SDNN, RMSSD, pNN50) and HEP amplitudes (N1 and P1), separately for the high and low emotionally dysregulated (HD and LD) groups.

Overall, most correlations did not reach statistical significance. However, one correlation emerged within the HD group, that is, SDNN was significantly positively correlated with the P1 component of the HEP ( $\rho = 0.44$ ,  $p = 0.04$ ), suggesting that individuals with greater heart rate variability, often interpreted as better autonomic flexibility, exhibited stronger late interoceptive cortical responses. This relationship was not observed in the LD group ( $\rho = -0.21$ ,  $p = 0.32$ ), hinting at a possible group-specific modulation (Table 6).

These results suggest that autonomic–cortical coupling, especially between SDNN and P1, may play a more prominent role in emotionally dysregulated individuals and could reflect differential regulation or integration of interoceptive signals at the cortical level in this sample.

HEP Component	HRV Metric	Spearman's $\rho$ Low Group	Spearman's $\rho$ High Group	Fisher's z-transformation	p
N1	MeanHR	-0.11	0.15	-0.81	0.42
P1	MeanHR	-0.18	-0.20	0.06	0.95
N1	RMSSD	0.36	-0.16	1.70	0.09
P1	RMSSD	-0.15	0.37	-1.67	0.10
N1	SDNN	0.30	-0.27	1.84	0.07
<b>P1</b>	<b>SDNN</b>	<b>-0.21</b>	<b>0.44</b>	<b>-2.14</b>	<b>0.03*</b>
N1	pNN50	0.32	-0.07	1.26	0.21
P1	pNN50	-0.11	0.24	-1.14	0.25

**Table 6** Correlations Between HEP Amplitudes and HRV Indices in High (HD) and Low (LD) Dysregulation Groups. Values represent Spearman's rho ( $\rho$ ) coefficients. Fisher's z transformation tested group differences. HR = heart rate; HRV = heart rate variability; SDNN = standard deviation of NN intervals; RMSSD = root mean square of successive differences; pNN50 = percentage of successive intervals differing by >50 ms. Significant correlations are highlighted in bold.

### 3.4.6 HR, HRV, and Questionnaires

We also explored correlations between cardiac measures (HR and HRV indices) and psychological questionnaire scores (UPPS-P, ALS-18, and STAI-Trait) across both groups. Although certain correlations showed moderate descriptive trends (e.g., negative correlation between impulsivity and MeanHR in the HD group:  $\rho = -0.49$ ), none reached statistical significance (Table 7). These results suggest limited direct associations between cardiac autonomic measures and psychological traits in this sample.

Questionnaire	HRV Metric	Spearman's $\rho$ Low Group	Spearman's $\rho$ High Group	Fisher's z transformation	p
<b>ALS-18</b>	MeanHR	-0.12	-0.25	0.44	0.66
	RMSSD	0.13	0.27	-0.44	0.66
	SDNN	0.09	0.28	-0.62	0.53
	pNN50	0.23	0.32	-0.30	0.76
<b>STAI-Trait</b>	MeanHR	-0.03	0.18	-0.64	0.52
	RMSSD	0.16	-0.13	0.92	0.36
	SDNN	0.19	-0.14	1.07	0.28
	pNN50	0.16	-0.08	0.75	0.45
<b>UPPS-P</b>	MeanHR	-0.07	-0.49	1.45	0.15
	RMSSD	-0.04	0.19	-0.72	0.47
	SDNN	-0.15	0.15	-0.93	0.35
	pNN50	-0.01	0.36	-1.21	0.23

**Table 7** Correlations Between Questionnaire Scores and HRV Indices in High (HD) and Low (LD) Dysregulation Groups. Values represent Spearman's rho ( $\rho$ ) coefficients. Fisher's z transformation tested group differences. ALS-18 = Affective Lability Scale-18; STAI-T = State-Trait Anxiety Inventory, Trait version; UPPS-P = Urgency, Premeditation, Perseverance, Sensation Seeking, and Positive Urgency scale. HRV = heart rate variability; HR = heart rate; SDNN = standard deviation of NN intervals; RMSSD = root mean square of successive differences; pNN50 = percentage of successive intervals differing by >50 ms.

## Chapter 4 - Discussion

### 4.1 Main HEP effects

This study found differences in heartbeat-evoked potentials between women with high and low emotional dysregulation. The HD group showed stronger early negativity (N1, 150 - 250 ms) and weaker later positivity (P1, 300 - 400 ms), while the LD group had stronger late responses, reflected in a GFP increase around 300 - 400 ms. GFP indicates the overall strength of brain activity independent of scalp location, suggesting that LD individuals recruit more globally synchronized areas during later stages of interoceptive processing.

These results fit with earlier studies showing that HEP components unfold in time. The early response (150 - 250 ms) reflects the brain's initial registration of cardiac signals (Park & Blanke, 2019), while the later response (300 - 400 ms) is linked to higher-order processing and conscious awareness of the body.

This distinction fits Craig's neuroanatomical model (2002; 2008), which proposes that cardiac signals move from spinal pathways (lamina I) to the insula, where they are transformed into subjective feelings and self-related representations. Other authors also stress that interoception is not only for homeostasis but also shapes emotions and cognition (Critchley & Garfinkel, 2017).

Our data suggest that women with high emotional dysregulation show stronger early but weaker late HEP responses. This means they may register visceral signals normally, or even more strongly, but have trouble carrying them into higher levels of processing. This fits multidimensional models of interoception (Ibáñez et al., 2020; Khalsa et al., 2018), which argue that dysfunction can appear at different stages, from basic detection to conscious awareness and emotional meaning. In this study, the reduced amplitude of the late HEP and GFP component in the HD group may indicate difficulties in turning bodily signals into stable emotional representations, contributing to problems with regulating emotions.

## **4.2 Trait associations (UPPS-P, STAI-T, ALS-18)**

### **4.2.1 Impulsivity (UPPS\_P)**

In the HD group, higher UPPS-P scores were positively correlated with early HEP (N1, 150 - 250 ms) and negatively with late HEP (P1, 300 - 400 ms). This suggests stronger early registration of cardiac signals but weaker later evaluative control. Referring to a study by Rapp et al. (2023), where adolescents with more ADHD symptoms (a construct with substantial impulsivity) showed elevated early HEPs, interpreted as heightened precision for internal bodily signals. Theoretical accounts of interoceptive predictive coding propose that impulsivity reflects over-weighting bottom-up visceral input alongside under-engagement of higher-order models and inhibitory control (Paulus & Stein, 2010; Owens et al., 2018; Tsakiris & Critchley, 2016). Converging evidence further links interoceptive processing to impulsivity phenotypes (Herman, 2019; Baiano et al., 2021), aligning with our results that impulsivity is characterized by early hyper-reactivity to bodily cues coupled with reduced late consolidation that would typically support context updating and self-regulation.

### **4.2.2 Trait anxiety (STAI-T)**

In our non-clinical sample of young women, within the HD subgroup, higher trait anxiety (STAI-T) was positively correlated with the early HEP (N1, 150–250 ms) and negatively correlated with the late HEP (P1, 300–400 ms) at CP1. In the same logic, anxiety reflects hypervigilant early detection of interoceptive signals, but under-engagement of later, integrative, as proposed in predictive coding accounts of interoception (Paulus & Stein, 2010; Owens et al., 2018). This aligns with neuroanatomical and functional models in which interoceptive inputs ascend to the insula and related regions to support conscious feelings and regulation (Craig, 2002, 2008; Park & Blanke, 2019). HEP studies in anxiety report altered cardiac-evoked responses (e.g., GAD and adrenergic manipulation), consistent with exaggerated early responses and weaker late integration (Pang et al., 2019; Verdonk et al., 2024; Quadt et al., 2018). Our findings, therefore, converge with a growing body of evidence, suggesting that anxiety, even at subclinical levels, alters the balance between early sensory precision and later appraisal of bodily signals, potentially contributing to maladaptive emotional experience in individuals with high emotional dysregulation.

### **4.2.3 Affective lability (ALS-18)**

In the HD group, higher affective lability (ALS-18) was positively correlated with early HEP (N1, 150 – 250ms) and negatively correlated with late HEP (P1, 300 – 400ms) at CP1, while no clear effects appeared in the LD group. This suggests that emotional instability is tied to weaker cortical evaluation of interoceptive signals in later processing. Affective lability is a transdiagnostic marker of vulnerability, strongly associated with emotional dysregulation and risk for psychiatric disorders (Dieujuste et al., 2025). Our result fits theories that unstable affective states may involve stronger early reactivity but weaker late appraisal of internal signals (Critchley & Garfinkel, 2017). Within predictive coding accounts (Owens et al., 2018; Ibáñez et al., 2020), this could reflect difficulties updating interoceptive predictions during emotional shifts. Although preliminary, these findings suggest that late HEPs may index how affective lability shapes interoceptive integration in young women. Future studies with larger and clinical samples, such as borderline personality disorder (Flasbeck et al., 2020), are needed to examine whether changes in P1 reliably index affective lability across clinical groups.

### **4.3 Between-questionnaire overlap (transdiagnostic)**

The strong correlations between impulsivity, affective lability, and trait anxiety suggest that these traits reflect overlapping aspects of emotional dysregulation. Prior work has shown that impulsivity often co-occurs with emotional instability and predicts vulnerability to mood and anxiety disorders (Whiteside & Lynam, 2001). Likewise, affective lability has been linked to higher anxiety and difficulties in emotional regulation (Henry et al., 2001). These associations point to shared regulatory mechanisms, where instability in processing and integrating internal signals contributes to both anxious tendencies and impulsive behavior. Such overlap supports the idea that different self-report constructs are tapping into interconnected aspects of the same underlying vulnerability. When considered together with the HEP findings, the results point to a transdiagnostic mechanism in which heightened early interoceptive reactivity and diminished late integration mirror the psychological profile of individuals prone to instability, impulsivity, and anxiety.

#### **4.4 HRV context and neurovisceral integration**

In the HD group, SDNN was positively correlated with P1 amplitude at CP1, suggesting that greater beat-to-beat variability was linked to stronger late HEP responses. No such effect appeared in the LD group. This aligns with evidence that HRV relates to cortical interoceptive markers, such as baseline HRV correlating with HEP amplitudes in clinical samples (Flasbeck et al., 2020). Since SDNN reflects overall autonomic flexibility (Shaffer & Ginsberg, 2017), its association with P1 supports neurovisceral-integration accounts, where higher HRV indicates more adaptive regulation. In this view, stronger late HEP components may index more effective cortical integration of bodily signals (Park & Blanke, 2019). That this effect emerged only in the HD group suggests that autonomic flexibility may modulate cortical integration of visceral signals when dysregulation is present.

## Chapter 5 - Limitations

Some observed features did not reach statistical significance, which is likely related to the limited sample size, the use of a sub-clinical female population, and the variability inherent to resting-state data. Moreover, the choice of CP1 as the electrode of interest was based on prior literature but not preregistered, which raises the possibility of ROI circularity. In addition, we relied on sensor-level analysis at centro-parietal sites without source localization, which limits the interpretation of the underlying neural regions.

Methodological aspects such as differences in epoch counts, fixed time windows, and variability in protocols across studies may also have influenced the results. Finally, we were unable to directly assess interoceptive accuracy through behavioral tasks (e.g., heartbeat counting or discrimination), therefore also the interpretation of the meaning of the early and late components is partially limited by it.

Future studies could extend this protocol to clinical populations and to male participants, where gender differences are expected. Including both frontal and centro-parietal regions, adopting source-localized analyses, and monitoring physiological covariates (e.g., respiration, cardiac phase) would improve sensitivity and interpretability. Standardized and preregistered protocols will also be important to validate and extend these findings across samples.

## Chapter 6 – Conclusion

At rest, women with higher emotion dysregulation displayed a distinct HEP profile over centro-parietal sites. Within this group, anxiety, impulsivity, and affective lability were positively associated with early (N1) and negatively with late (P1) responses. This “early strong, late weak” configuration may provide an organizing principle for resting-state interoception in dysregulation and suggests that HEPs capture meaningful individual differences.

The strong correlations observed among anxiety, impulsivity, and affective lability further support the view that these traits represent interconnected dimensions of dysregulation, rather than isolated constructs. Their convergence with the HEP pattern strengthens the case for HEPs as a potential neural marker. Although a positive SDNN and P1 association was also observed, this was the only significant cardiac effect, indicating that autonomic variability may provide a supportive context but is not essential. Taken together, these results suggest that HEP measures, particularly the N1 and P1 dissociation, may provide a sensitive index of ED-related traits at rest, although replication is needed to establish their reliability and specificity.

Future research should standardize analytic pipelines (e.g., predefined N1 and P1 windows and centro-parietal or frontal clusters), evaluate reliability, and examine generalizability across sites and populations, including males and clinical groups. Importantly, specificity and predictive value should be tested, particularly whether baseline HEPs can forecast changes in dysregulation or track intervention effects. If validated, resting HEPs, especially the N1 and P1 dissociation, may serve as a physiologically interpretable neural marker for identifying and monitoring emotion dysregulation over time.

## References:

1. Nayok, S. B., Sreeraj, V. S., Shivakumar, V., & Venkatasubramanian, G. (2023). A Primer on Interoception and its Importance in Psychiatry. *Clinical Psychopharmacology and Neuroscience*, 21(2), 252.
2. Tsakiris, M., & Critchley, H. (2016). Interoception beyond homeostasis: affect, cognition, and mental health. *Philosophical Transactions of the Royal Society B: Biological Sciences*, 371(1708), 20160002.
3. Craig, A. D. (2002). How do you feel? Interoception: the sense of the physiological condition of the body. *Nature reviews neuroscience*, 3(8), 655-666.
4. Fittipaldi, S., Abrevaya, S., de la Fuente, A., Pascariello, G. O., Hesse, E., Birba, A., ... & Ibáñez, A. (2020). A multidimensional and multi-feature framework for cardiac interoception. *Neuroimage*, 212, 116677.
5. Critchley, H. D., & Garfinkel, S. N. (2017). Interoception and emotion. *Current opinion in psychology*, 17, 7-14.
6. Craig, A. D. (2008). Interoception and emotion: a neuroanatomical perspective. *Handbook of emotions*, 3(602), 272-88.
7. Khalsa, S. S., Adolphs, R., Cameron, O. G., Critchley, H. D., Davenport, P. W., Feinstein, J. S., ... & Zucker, N. (2018). Interoception and mental health: a roadmap. *Biological psychiatry: cognitive neuroscience and neuroimaging*, 3(6), 501-513.
8. Engelen, T., Solcà, M., & Tallon-Baudry, C. (2023). Interoceptive rhythms in the brain. *Nature Neuroscience*, 26(10), 1670-1684.
9. Park, H. D., & Blanke, O. (2019). Heartbeat-evoked cortical responses: Underlying mechanisms, functional roles, and methodological considerations. *NeuroImage*, 197, 502-511.
10. Quadt, L., Critchley, H. D., & Garfinkel, S. N. (2018). The neurobiology of interoception in health and disease. *Annals of the New York Academy of Sciences*, 1428(1), 112-128.
11. Paulus, M. P., & Stein, M. B. (2010). Interoception in anxiety and depression. *Brain structure and Function*, 214(5), 451-463.
12. Dieujeste, N., Petri, J. M., Mekawi, Y., Lathan, E. C., Carter, S., Bradley, B., ... & Powers, A. (2025). Investigating associations between emotion dysregulation and DSM-5 posttraumatic stress disorder (PTSD) using network analysis. *Journal of Affective Disorders*, 377, 106-115.

12. Barnes, G. L., Ozsivadjian, A., Baird, G., Absoud, M., & Hollocks, M. J. (2025). Investigating The effects of transdiagnostic processes on anxiety and depression symptoms in autistic young people: The mediating role of emotion dysregulation. *Journal of Autism and Developmental Disorders*, *55*(3), 969-980.
13. Chan, K. M., Hong, R. Y., Ong, X. L., & Cheung, H. S. (2023). Emotion dysregulation and symptoms of anxiety and depression in early adolescence: Bidirectional longitudinal associations and the antecedent role of parent–child attachment. *British Journal of Developmental Psychology*, *41*(3), 291-305.
14. Herber, C. L., Breuninger, C., & Tuschen-Caffier, B. (2025). Psychophysiological stress response, emotion dysregulation and sleep parameters as predictors of psychopathology in adolescents and young adults. *Journal of Affective Disorders*, *375*, 331-341.
15. Bender, P. K., Reinholdt-Dunne, M. L., Esbjørn, B. H., & Pons, F. (2012). Emotion dysregulation and anxiety in children and adolescents: Gender differences. *Personality and Individual Differences*, *53*(3), 284-288.
16. Schulz, A., & Vögele, C. (2015). Interoception and stress. *Frontiers in psychology*, *6*, 993.
17. Owens, A. P., Allen, M., Ondobaka, S., & Friston, K. J. (2018). Interoceptive inference: From computational neuroscience to clinic. *Neuroscience & Biobehavioral Reviews*, *90*, 174-183.
18. Tummeltshammer, K., Feldman, E. C., & Amso, D. (2019). Using pupil dilation, eye-blink rate, and the value of mother to investigate reward learning mechanisms in infancy. *Developmental cognitive neuroscience*, *36*, 100608.
19. Min, J., Yu, J., Chae, Y., & Lee, J. H. (2023). Sex differences in interoceptive sensitivity and the neural correlates during emotional processing. *Frontiers in Neuroscience*, *17*, 1022153. <https://doi.org/10.3389/fnins.2023.1022153>
20. Fusina, F., Marino, M., Spironelli, C., & Angrilli, A. (2022). Ventral attention network correlates with high traits of emotion dysregulation in community women—a resting-state EEG study. *Frontiers in Human Neuroscience*, *16*, 895034.
21. Herman, A. M., Rae, C. L., Critchley, H. D., & Duka, T. (2019). Interoceptive accuracy predicts nonplanning trait impulsivity. *Psychophysiology*, *56*(6), e13339.
22. Poppa, T., Benschop, L., Horczak, P., Vanderhasselt, M. A., Carrette, E., Bechara, A., ... & Vonck, K. (2022). Auricular transcutaneous vagus nerve stimulation modulates the heart-evoked potential. *Brain Stimulation*, *15*(1), 260-269..

23. Taberna, G. A., Samogin, J., Zhao, M., Marino, M., Guarnieri, R., Morales, E. C., ... & Mantini, D. (2024). Large-scale analysis of neural activity and connectivity from high-density electroencephalographic data. *Computers in biology and medicine*, *178*, 108704.
24. Marino, M., Liu, Q., Koudelka, V., Porcaro, C., Hlinka, J., Wenderoth, N., & Mantini, D. (2018). Adaptive optimal basis set for BCG artifact removal in simultaneous EEG-fMRI. *Scientific reports*, *8*(1), 8902.
25. Baiano, C., Santangelo, G., Senese, V. P., Di Mauro, G., Lauro, G., Piacenti, M., & Conson, M. (2021). Linking perception of bodily states and cognitive control: the role of interoception in impulsive behaviour. *Experimental Brain Research*, *239*(3), 857-865.
26. M. Bruton, A., Levy, L., Rai, N. K., Colgan, D. D., & M. Johnstone, J. (2025). Diminished Interoceptive Accuracy in Attention-Deficit/Hyperactivity Disorder: A Systematic Review. *Psychophysiology*, *62*(2), e14750.
27. Herman, A. M. (2023). Interoception within the context of impulsivity and addiction. *Current addiction reports*, *10*(2), 97-106.
28. Hebb, D. O. (1955). Drives and the CNS (conceptual nervous system). *Psychological review*, *62*(4), 243.
29. Jenkinson, P. M., Fotopoulou, A., Ibañez, A., & Rossell, S. (2024). Interoception in anxiety, depression, and psychosis: a review. *EClinicalMedicine*, *73*.
30. Al, E., Iliopoulos, F., Forschack, N., Nierhaus, T., Grund, M., Motyka, P., ... & Villringer, A. (2020). Heart–brain interactions shape somatosensory perception and evoked potentials. *Proceedings of the National Academy of Sciences*, *117*(19), 10575-10584.
31. Flasbeck, V., Popkirov, S., Ebert, A., & Brüne, M. (2020). Altered interoception in patients with borderline personality disorder: a study using heartbeat-evoked potentials. *Borderline Personality Disorder and Emotion Dysregulation*, *7*(1), 24.
32. Look, A. E., Flory, J. D., Harvey, P. D., & Siever, L. J. (2010). Psychometric properties of a short form of the Affective Lability Scale (ALS-18). *Personality and Individual Differences*, *49*(3), 187-191.
33. Terhaar, J., Viola, F. C., Bär, K. J., & Debener, S. (2012). Heartbeat evoked potentials mirror altered body perception in depressed patients. *Clinical neurophysiology*, *123*(10), 1950-1957.

34. Pang, J., Tang, X., Li, H., Hu, Q., Cui, H., Zhang, L., ... & Li, C. (2019). Altered interoceptive processing in generalized anxiety Disorder—A Heartbeat-Evoked potential research. *Frontiers in psychiatry*, *10*, 616.
35. Rapp, L., Mai-Lippold, S. A., Georgiou, E., & Pollatos, O. (2023). Elevated EEG heartbeat-evoked potentials in adolescents with more ADHD symptoms. *Biological Psychology*, *184*, 108698.
36. Müller, L. E., Schulz, A., Andermann, M., Gäbel, A., Gescher, D. M., Spohn, A., ... & Bertsch, K. (2015). Cortical representation of afferent bodily signals in borderline personality disorder: neural correlates and relationship to emotional dysregulation. *JAMA psychiatry*, *72*(11), 1077-1086.
37. Shaffer, F., & Ginsberg, J. P. (2017). An overview of heart rate variability metrics and norms. *Frontiers in public health*, *5*, 258.
38. Koval, P., Ogrinz, B., Kuppens, P., Van den Bergh, O., Tuerlinckx, F., & Sütterlin, S. (2013). Affective instability in daily life is predicted by resting heart rate variability. *PloS one*, *8*(11), e81536.
39. Fló, E., Belloli, L., Cabana, Á., Ruyant-Belabbas, A., Jodaitis, L., Valente, M., ... & Sitt, J. (2024). Predicting attentional focus: Heartbeat-evoked responses and brain dynamics during interoceptive and exteroceptive processing. *PNAS nexus*, *3*(12), pgae531.
40. Zaccaro, A., Della Penna, F., Mussini, E., Parrotta, E., Perrucci, M. G., Costantini, M., & Ferri, F. (2024). Attention to cardiac sensations enhances the heartbeat-evoked potential during exhalation. *IScience*, *27*(4).
41. Verdonk, C., Teed, A. R., White, E. J., Ren, X., Stewart, J. L., Paulus, M. P., & Khalsa, S. S. (2024). Heartbeat-evoked neural response abnormalities in generalized anxiety disorder during peripheral adrenergic stimulation. *Neuropsychopharmacology*, *49*(8), 1246-1254.
42. Marino, M., Liu, Q., Koudelka, V., Porcaro, C., Hlinka, J., Wenderoth, N., & Mantini, D. (2018). Adaptive optimal basis set for BCG artifact removal in simultaneous EEG-fMRI. *Scientific reports*, *8*(1), 8902.
43. Whiteside, S. P., & Lynam, D. R. (2001). The five factor model and impulsivity: Using a structural model of personality to understand impulsivity. *Personality and individual differences*, *30*(4), 669-689.
44. Henry, C., Mitropoulou, V., New, A. S., Koenigsberg, H. W., Silverman, J., & Siever, L. J. (2001). Affective instability and impulsivity in borderline personality and bipolar

II disorders: similarities and differences. *Journal of psychiatric research*, 35(6), 307-312.

45. Liu, H., Liang, H., Yu, X., Wang, G., Han, Y., Yan, M., ... & Wang, W. (2023). Enhanced external counterpulsation modulates the heartbeat evoked potential. *Frontiers in physiology*, 14, 1144073.
46. Carlson, S. R., & Tháí, S. (2010). ERPs on a continuous performance task and self-reported psychopathic traits: P3 and CNV augmentation are associated with Fearless Dominance. *Biological psychology*, 85(2), 318-330.